

# NUMERICAL ANALYSIS OF MELTING MECHANISM IN A RECTANGULAR THERMAL ENERGY STORAGE

**<sup>1</sup>Reema Jadhav, <sup>2</sup>Prof.S.Y.Bhosale, <sup>3</sup>Prof. A.V. Waghmare and <sup>4</sup>Prof. H.N. Deshpande**

<sup>1</sup>Student of Department of Mechanical Engineering, PES's Modern college of Engineering, Pune, India.

<sup>2</sup>Department of Mechanical Engineering, PES's Modern college of Engineering, Pune, India.

<sup>3</sup>Department of Mechanical Engineering, AISSMS College of EngineeringPune, India.

<sup>4</sup>Department of Mechanical Engineering, PES's Modern college of Engineering, Pune, India.

**Abstract—** In this research work, investigation of the impact of Phase Change Material concentration, thermal conditions surrounding the Thermal Energy Storage System for the charging and discharging process was conducted by including  $Al_2O_3$  as nano-material with a varying concentration – 0% (Base Model), 1% (Variant-1), 2% (Variant-2) and 3% (Variant-3). Three thermal conditions surrounding the TESS were studied – complete insulation (Configuration A), atmospheric condition on one side (Configuration B), partial exposure (Configuration C). These were studied using experimental and CFD methods for two heat loads 125 W and 175 W. Transient, 3-Dimensional, Laminar CFD simulations were conducted using ANSYS FLUENT with the Enthalpy-Porosity approach. For Configuration A under the heat load of 125 W, Variant-1 had high temperature at the monitoring-point followed up by the Variant-2. When the environmental conditions were imposed on the opposing wall of the heat supply (Configuration B) of 125 W, the melting inside the TESS monitoring-point had occurred at 24 minute for the Variant-1. For the Configuration C under 175 W, the peak temperature of 400 K was observed for the Variant-1. When the heat supply was increased to 175 W from 125 W for the Configuration A, the melting initiation at the monitoring-point had occurred faster. Overall, the inclusion of nano-materials with the PCMs had resulted in this thermal advantage.

**Keywords:** PCMs, TESS, Melting, nano-materials, CFD Methods

## I. INTRODUCTION

The necessity of energy source for the human kind' survival and further technological developments is very crucial. At present, fossil fuels accounts for major part of the energy source that had been used worldwide. Although majority of the world's population depend on the fossil fuels for the day to day activities, the emerging concerns over the pollution from these type of fuels are of concern for global climate changes. Also, in the long term, the availability of these fuels could be reduced as these are non-renewable energy sources.

In order to improve the utilization of the available energy, continuous research had been focused on energy storage mechanisms. There have been two major thermal energy storage systems – Sensible Heat Storage (SHS) and Latent Heat Storage (LHS). In the latent heat storage systems, the thermal energy released during the phase change process will be stored. This can be explained using the following example. The phase change materials such as Paraffin Wax will melt to the liquid state during the heat supply such as Solar radiation in the day time. During the solidification process, such as in the colder temperature of night time, the energy released could be utilized for heating purposes.

Sina Lohrasbi et.al<sup>[1]</sup> had investigated the methods to optimize the discharging process of latent heat thermal storage system (LHTESS) with the help of V-shaped fins. In the discharging process, the expedition of the solidification process is critical and the authors had included the solidification expedition and maximum energy storage capacity as the primary variables in their study. The impact of thermo-physical properties of the PCM with the dispersion of nano-particles ( $TiO_2$ ) was studied by R. K. Sharma et.al<sup>[2]</sup>. They had considered Palmitic Acid as the PCM with 0.5, 1.3 and 5% mass fraction of  $TiO_2$  in their study. Nitesh Das et.al<sup>[3]</sup> had modeled the vertically oriented latent heat thermal energy storage system as 2-dimensional axi-symmetric in their CFD simulations. The melting process of PCMs were simulated using the enthalpy-porosity method. The inclusion of the Graphene in to the PCMs resulted in reduction of melting rate by upto 22%. The impact of the orientation – vertical and horizontal – in a shell-and-tube thermal storage system was studied by Saeid Seddigh et.al<sup>[4]</sup>. Based on the results from their study, they had concluded that the horizontal unit to be effective for the charging process, when the top half melts. However, the effectiveness of the horizontal unit to reduced when the bottom half melts during the charging process. Rasool Kalbasi et.al<sup>[5]</sup> had conducted optimization study for heat removal from portable electronic components with the help of thermal energy storage systems. They had compared the thermal performance for a rectangular and square shaped TESS for the identical operating conditions. They had identified that the rectangular TESS provided better performance in terms of melting time as compared to the square TESS. A mixture of Sodium Nitrate and Potassium Nitrate as the PCM in a thermal storage system that was under the natural convection effects was studied by J Vogel et.al<sup>[6]</sup>. In their study, the simulations were performed using the enthalpy-porosity technique. By this approach, the complexities that are associated with multi-phase simulations are avoided. A finite volume based numerical simulation for investigating the charging process in a horizontally placed tube was conducted by Kamal A R Ismail et.al<sup>[7]</sup>. The authors had developed the numerical solver for this 2-dimensional geometry. The results obtained from these simulations were compared against the experimental data for validation. For this transient simulations, the authors had identified 0.01 s as time-step size. D. Cano et.al<sup>[8]</sup> had studied the heat recovery from a hydrogen cycle's residual energy with the help of a tube-in-tube heat exchanger that utilized thermal energy storage system. They conclude that the countercurrent mode of operation resulted in efficient energy transfer in the tube-in-tube heat exchanger thermal energy storage system. Thermal conductivity enhancement for the Lauric Acid – to be used as PCM – was investigated by Sivasankaran Harish et.al<sup>[9]</sup>. The authors had added Graphene Nano-Platelets (GNP) of 5-10 nm in size with the Lauric Acid in order to enhance the thermal conductivity of the PCMs. The synthesis of Lauric Acid in to the porous Expanded Vermiculite (EVM) as form stable PCM was studied by Rulong Wen et.al<sup>[10]</sup>. This resulted in Lauric Acid as PCM while Expanded Vermiculite (EVM) was acting as the supporting material. With this synthesis, the stability of PCM was found to be increasing. Reema Jadhav et.al<sup>[11]</sup> studied selection of Phase Change material, selection of nanomaterial and stability of nanomaterial.

## II. NUMERICAL ANALYSIS

A TESS of rectangular cross section with a dimension of 50 mm X 200 mm X 80 mm was considered for this research work. The CAD model of the TESS for this dimension was built using ANSYS Design Modeler and shown below in figure 1.

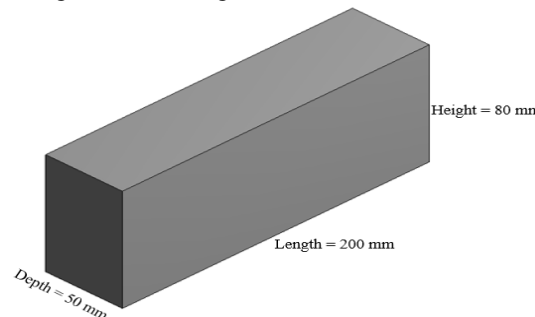


Fig.1: CAD model for the TESS

This thermal energy storage system had been filled up with the phase change material (PCM) of paraffin wax at a solid state. The heat input to the TESS was supplied through the electrical energy in the experimental studies. For this project work, the two thermal loads were investigated 125 W and 175 W. This heat load was applied over a surface of 200 mm X 80 mm cross-section as shown in the following figure, colored in Blue.

Three configurations – Configurations A, B and C – were defined based on the thermal loads and thermal conditions. The heat supply area for the Configuration A and Configuration B were the same. But, for the Configuration C, the heat supply area was 100 mm X 80 mm, half of the heat supply area from Configuration A and B. With this partial heating for the identical heat supply, the PCM melting rate as well as melting time was expected to be influenced. And, investigation of this particular mechanism was one the primary objective of this research work.

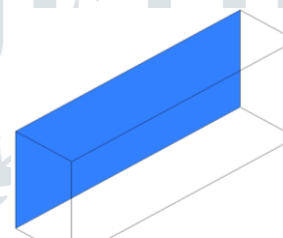


Fig.2: Configuration – A

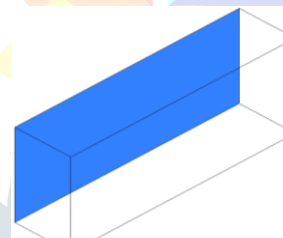


Fig.3: Configuration – B

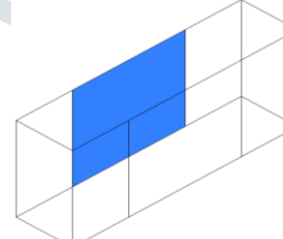


Fig.4: Configuration – C

The major focus of this research was to study the factors that influence the melting and solidification process. One of such factor was the atmospheric conditions that surrounds the thermal energy storage systems (TESS). Heat loss from the TESS to the surrounding would delay the melting process while the melting could be accelerated if there had been a heat gain from the surrounding to the TESS. In this research work, this was studied by applying three thermal conditions.

**Case 1: Adiabatic conditions on TESS boundaries**

Under this conditions, the TESS was assumed to be sufficiently insulated that there were no heat transfer between the surrounding (atmospheric conditions) and the TESS.

**Case 2: atmospheric temperature on the opposing wall**

For these thermal conditions, the wall opposite to the heat supplying surface was applied with surrounding temperature (300 K) while the remaining TESS surfaces were sufficiently insulated to prevent any heat transfer between the surrounding and the TESS.

**Case 3: Partial exposure**

The impact of partial exposure to the surrounding was studied here, with half of the surface area as compared to the previous case was exposed to atmosphere (300 K).

The melting and solidification characteristics of the phase change materials (PCMs) has a major role in terms of the thermal energy storage systems (TESS)' performance. Even though paraffin wax has high energy storage, its thermal conductivity was of lower. Various researchers had suggested the mixing of nano-materials such as Al<sub>2</sub>O<sub>3</sub> in to the paraffin wax to enhance the thermal conductivity. The concentration of the nano-materials could alter the charging-discharging mechanisms in the TESS.

### III. COMPUTATIONAL METHODOLOGY

A geometrical model with those dimensions was built in Design Modeler and was meshed in ANSYS Mesher with the help of Sweep Mesh Methods.

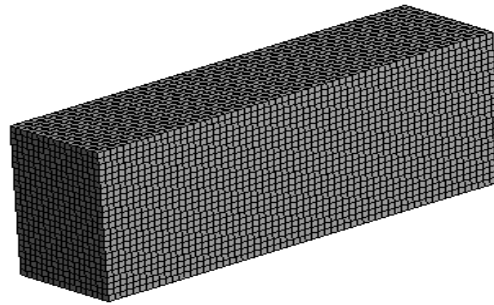


Fig.5: Meshing for the TESS

Total mesh count was 24,800 for this thermal energy storage system geometry. These transient simulations were performed using the pressure-based solver in ANSYS FLUENT to account for the incompressible flows. The gravitational effects for this simulations. Since the overall flow motion during the melting would be largely gravity-driven, flow turbulence would be absent. So, laminar solver was applied for this study. In the CFD simulations, wall boundary condition with constant heat flux was employed to apply the heat load as shown in the figure RJ. For the remaining boundaries, adiabatic conditions were applied by specifying heat flux = 0 W/m<sup>2</sup>. For the Configuration B and C, constant temperature of 300 K was applied for the atmospheric conditions. The pressure-velocity coupling for solving the incompressible flows with the pressure-based solver was achieved using PISO scheme. Second-order discretization schemes were employed for spatial discretization for the improved accuracy.

### IV. RESULTS AND DISCUSSION

#### A. Pattern of solid-liquid interface

In the beginning of the melting, heating from side, conduction is the initial heat transfer mechanism. During the early stage, buoyancy forces cannot overcome the resistance imposed by the viscose forces. The isotherms, at the beginning of the melting process, are parallel to hot vertical side of the enclosure due to a dominating role of heat conduction. The effect of convection is seen as a departure of the isotherms from being parallel to the hot wall As time elapses, the deformation of the isotherms and then the interface liquid–solid becomes more accentuated and the mechanism of transfer of heat is gradually shifted to natural convection.

From the contour plots, high temperature was observed for all variants except Variant-3 after 15 minutes. The melting had begun from the heat supply wall and the PCMs at the interiors had also started to melt at 15 minutes. At 30 minutes, nearly half the PCM was melted for all the variants.

The melting profile from the liquid fraction indicate the melting rate, till this time period, was nearly similar. From the contours of liquid fraction at 60th minute, Variant-1 had complexly melted while the Base Model and Variants 1 and 3 show some residuals. Actually, the complete melting for the Variant-1 had occurred at 45th minute itself.

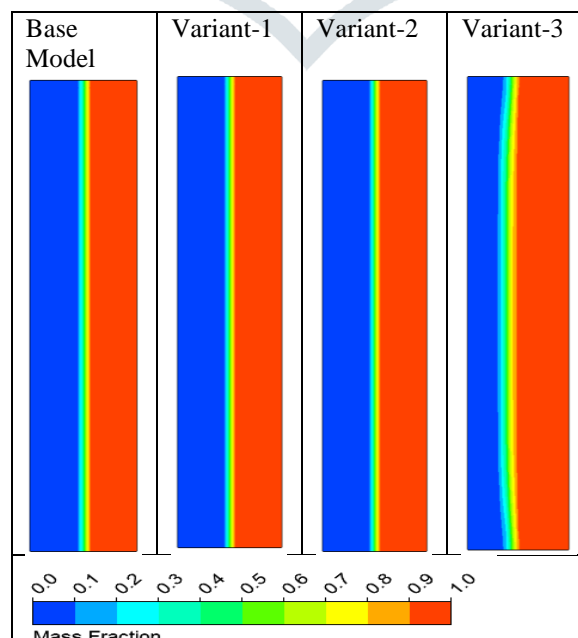


Fig.6: Liquid Fraction contours for Configuration-A (125 W) at Time = 30 minutes

This suggest that Variant-1 was better for thermal storage as compared to the remaining Variants. The inclusion of nano-materials resulted in enhanced performance of the PCM as against the pure Paraffin Wax (Base Model).

In the configuration B, the environmental condition of 300 K was applied to the opposite face of the heat input of TESS. From the contour plots, high temperature was observed for base model and variant-1 after 15 minutes. The melting had begun from the heat supply wall and the PCMs at the interiors had also started to melt at 15 minutes.

At 30 minutes, nearly half the PCM was melted for all the variants. The melting profile from the liquid fraction indicate the melting rate, till this time period, was nearly similar. From the contours of liquid fraction at 60 minutes, Variant-1 and variant-2 had complexly melted while the Base Model and Variants-3 show some residuals. This suggest that Variant-1 and variant-2 was better for thermal storage as compared to the remaining base model and Variant-3.

In the configuration C, partially heating was applied to the heat input of TESS.

The melting had begun from the heat supply wall and the PCMs at the interiors had also started to melt at 15 minutes. At 30 minutes, nearly the PCM was melted for all the variants except variant-2. At 45 minutes, nearly variant-2 also melted.

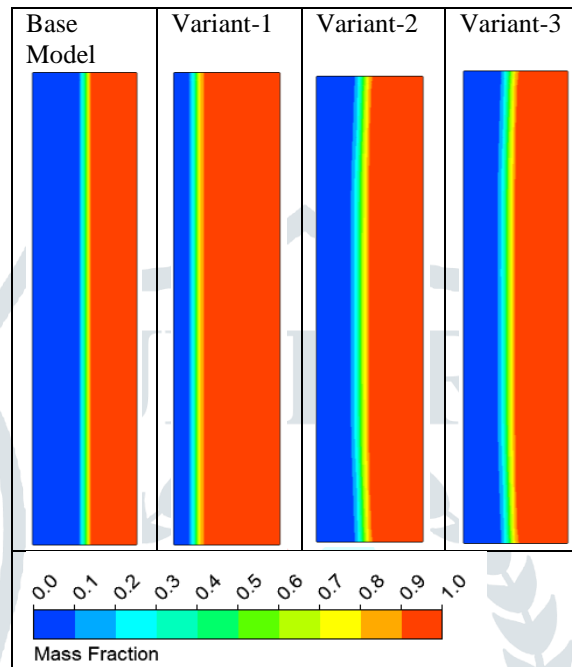


Fig.7: Liquid Fraction contours for Configuration-B (125 W) at Time = 30 minutes

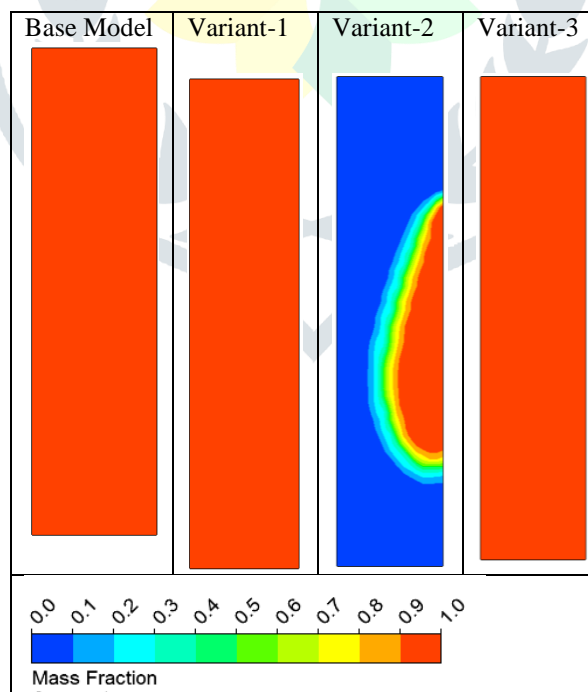


Fig.8: Liquid Fraction contours for Configuration-C (125 W) at Time = 30 minutes

For all configurations, the liquid fraction contour plots were shown for 30 minutes.

## B. Temperature Analysis

Variant-1 that had 1% Al<sub>2</sub>O<sub>3</sub>, showed higher temperature as compared to the remaining cases. Variant-2 had high temperature till ~25 minutes but higher temperature was observed for Variant-1 from 25 minutes onwards. So, the melting was first initiated, (Figure 12) at the monitoring-point, for Variant-2 however, complete melting occurred around 30 minutes for both Variant-1 and Variant-2.

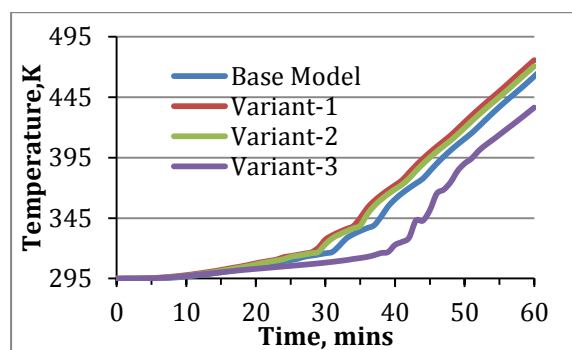


Fig.9: Temperature comparison at the monitoring-point for Configuration A, heat load = 125 W

In the configuration B , high temperature was observed for the Base Model and the Variant-1 at the monitoring-point. As compared to the Variant-2 and Variant-3, nearly 25% rise in temperature was noted at this point at time = 60 minutes. (Figure 10)

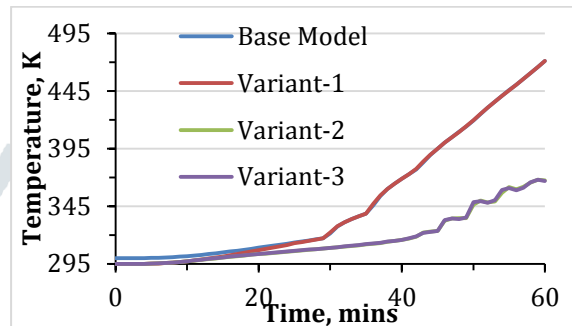


Fig.10: Temperature comparison at the monitoring-point for Configuration B, heat load = 125 W

In the configuration C, with the partial heating and partial convection conditions at the other side, the maximum temperature observed at the monitoring-point was lower (Figure 13) than the Configuration A and Configuration B under the same heat loads.

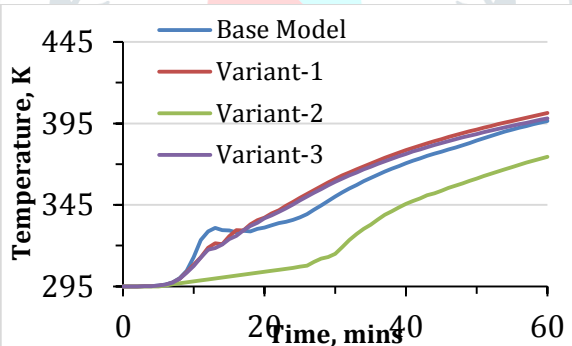


Fig.11: Temperature comparison at the monitoring-point for Configuration C, heat load = 125 W

The heat loss to the surrounding due to the convection conditions at the TESS was identified as the reason for this.

When the heat supply was increased to 175 W from 125 W, the melting initiation at the monitoring-point had occurred faster for all the three configurations that were studied in this research work. The Variant 1 showed accelerated melting (at 21 minutes) followed by Base Model (at 22 minutes) however Variant 2 and Variant 3 were observed to have delayed melting at the monitoring-point. For the Variant 2 and Variant 3, the melting was initiated around 28 minutes. (Figure 12)

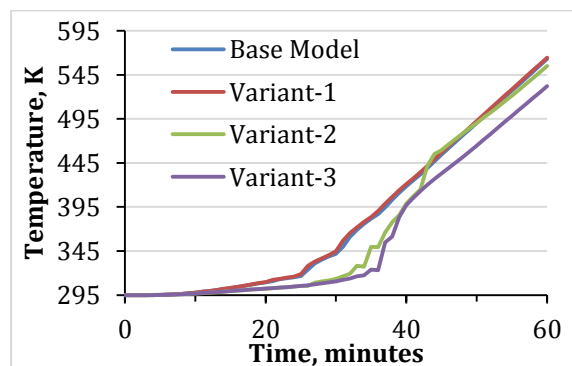


Fig.12: Temperature comparison at the monitoring-point for Configuration A, heat load = 175 W

For the Configuration B under 175 W of heat supply, the melting at the monitoring- point for the Base Model occurred at 22 minutes while for the Variant-1 the melting occurred at 22 minutes.

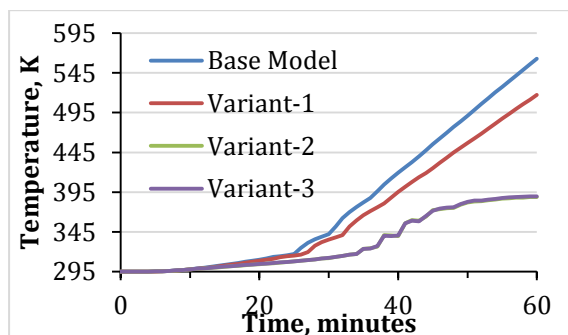


Fig.13: Temperature comparison at the monitoring-point for Configuration B, heat load = 175 W

However, the maximum temperature at the monitoring-point for the Base Model was 563 K but it was 518 K for the variant-1. It could be observed that the maximum temperature for these variants were ~395 K, significantly lower than the Base Model and Variant-1.

In Configuration C, the partial heating mechanism with a high heat load (175 W) ensured the faster melting and the PCM at the monitoring point began to melt as early 5 minutes for Variant-2. However, for the Base Model, the melting at the monitoring-point was initiated only from 25th minute. This indicates the advantages of the nano-particles in the PCMs.

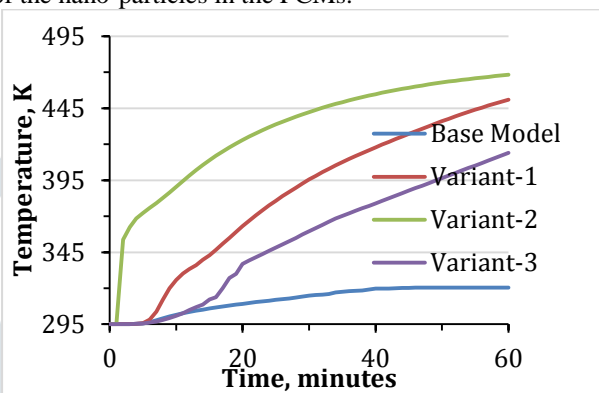


Fig.14: Temperature comparison at the monitoring-point for Configuration C, heat load = 175 W

## V CONCLUSION

- For Configuration A under the heat load of 125 W, Variant-1 and Variant-2 had high temperature as compared to the Base Model, (10 – 20 K). The inclusion of nano-materials with the PCMs had resulted in this thermal advantage.
- When the heat supply was increased to 175 W from 125 W for the Configuration A, the melting initiation at the monitoring-point had occurred faster. A similar trend was observed for the remaining two configurations as well.
- The thermal conditions surrounding the TESS such as adiabatic (Configuration A), environmental conditions (Configuration B) and partial heating and partial exposure (Configuration C) had strong influence on the melting mechanism of the TESS.
- Also, the PCM concentration had influenced the melting process based on these thermal conditions.

## REFERENCES

- Sina Lohrasbi, Mofid Gorji Bandpy, D D Ganji, "Response Surface Method Optimization of V-Shaped Fin Assisted Latent Heat Thermal Energy Storage System during Discharging Process" Alexandria Engineering Journal, Volume 55, pp 2065-2076, 2016;
- R K Sharma, P Ganesan, V V Tyagi, H S C Metselaar, S C Sandaran, "Thermal Properties and Heat Storage Analysis of Palmitic Acid-TiO<sub>2</sub> Composite as Nano-Enhanced Organic Phase Change Material (NEOPCM)" Applied Thermal Engineering, Volume 99, pp 1254-1262, 2016;
- Nitesh Das, Yasuyuki Takata, Masamichi Kohno, Sivasankaran Harish, "Melting of Graphene Based Phase Change Nono-Composites in Vertical Latent Heat Thermal Energy Storage Unit" Applied Thermal Engineering, Volume 107, pp 101-113, 2016;
- Saeid Seddegh, Xiaolin, Alan D Henderson, "A Comparative Study of Thermal Behavior of a Horizontal and Vertical Shell-and-Tube Energy Storage using Phase Change Materials" Applied Thermal Engineering, Volume 93, pp 348-358, 2016;
- Rasool Kalbasi, Mohammad Reza Salimpour, "Constructal Design of Phase Change Material Enclosure used for Cooling Electronic Devices" Applied Thermal Engineering, Volume 84, pp 339-349, 2015;
- J Vogel, J Felbinger, M Johnson, "Natural Convection in High Temperature Flat Plate Latent Heat Thermal Energy Storage Systems" Applied Energy, Volume 184, pp 184-196, 2016;
- Kamal A. R. Ismail, Fatima A. M. Lino, Raquel C. R. Da Silva, Antonio B. de Jesus, Louryval C Paixao, "Experimentally Validated Two-Dimensional Numerical Model for the Solidification of PCM Along a Horizontal Long Tube" International Journal of Thermal Sciences, Volume 75, pp 184-193, 2014;
- D. Cano, C. Funez, L. Rodriguez, J. L. Valverde, L. Sanchez-Silva, "Experimental Investigation of a Thermal Storage System using Phase Change Materials" Applied Thermal Engineering, Volume 107, pp 264-270, 2016;
- Sivasankaran Harish, Daniel Orejon, Yasuyuki Takata, Masamichi Kohno, "Thermal Conductivity Enhancement of Lauric Acid Phase Change Nano-Composite with Graphene Nano-Platelets" Applied Thermal Engineering, Volume 80, pp 205-211, 2015;
- Ruilong Wen, Zhaojun Huang, Yaoting Huang, Xiaoguang Zhang, Xin Min, Minghao Fang, Yangai Liu, Xiaowen Wu, "Synthesis and Characterization of Lauric Acid/Expanded Vermiculite as Form-Stabilized Thermal Energy Storage Materials" Energy and Buildings, Volume 116, pp 677-683, 2016;
- Reema R. Jadhav, Sameer. Y. Bhosale and A. V. Waghmare "Heat Transfer Enhancement during Charging and Discharging of Pure Paraffin Wax with Dispersion of Nanomaterial" International Engineering Research Journal (IERJ) Special Issue Page 788-792, June 2016, ISSN 2395-1621